World Journal of Advanced Research and Reviews
eISSN: 2581-9615 CODEN (USA): WJARAI
Cross Ref DOI: 10.30574/wjarr
Journal homepage: https://wjarr.com/

(RESEARCH ARTICLE)

Check for updates

Green synthesis of magnesium oxide nanoparticles from *Solanum lycopersicum* and evaluation of their antidiabetic effect in rats

Uma Priya L and John Sushma Nannepaga *

Department of Biotechnology, Sri Padmavati Mahila Visvavidyalayam, Tirupati, Andhra Pradesh, India.

World Journal of Advanced Research and Reviews, 2025, 26(03), 1380-1392

Publication history: Received on 03 April 2025; revised on 11 May 2025; accepted on 13 May 2025

Article DOI: https://doi.org/10.30574/wjarr.2025.26.3.1709

Abstract

This study investigates the green synthesis of magnesium oxide nanoparticles (MgO NPs) using *Solanum lycopersicum* (tomato) extract and evaluates their antidiabetic effect in rats. Diabetic neuropathy (DN) being the common and debilitating complication of diabetes mellitus was therapeutically targeted. The synthesized MgO NPs were characterized using UV-Vis spectrophotometry, phase contrast microscopy, FTIR, SEM-EDS, particle size and zeta potential analyser, and TEM. The antidiabetic neuropathic effect of the *Solanum lycopersicum*-derived MgO NPs was assessed in streptozotocin-induced diabetic rats by measuring biochemical parameters (blood glucose, HbA1c, and insulin levels), performing histopathological analysis of various brain regions, and conducting behavioral tests to evaluate nociception and motor activity. The results indicate the successful green synthesis of MgO NPs from *Solanum lycopersicum* and demonstrate their potential to ameliorate diabetic neuropathy in rats, suggesting a promising antidiabetic effect.

Keywords: Green Synthesis; Magnesium Oxide Nanoparticles (MgO NPs); *Solanum lycopersicum;* Antidiabetic Activity; Streptozotocin-Induced Diabetes

1. Introduction

Diabetes mellitus, particularly type 2 diabetes mellitus (T2DM), is a growing global health concern characterized by chronic hyperglycemia resulting from impaired insulin secretion, insulin resistance, or both. Persistent high blood glucose levels can lead to long-term damage to various organs, including the heart, kidneys, eyes, and blood vessels [1]. Despite the availability of numerous synthetic antidiabetic drugs, many suffer from limitations such as poor bioavailability, adverse side effects, high cost, and the need for long-term administration. As a result, there is increasing interest in alternative, safer, and more effective therapeutic strategies, including those derived from nanotechnology and medicinal plants [2].

Nanoparticles (NPs) have shown tremendous potential in the treatment of metabolic disorders due to their unique physicochemical properties, including high surface area-to-volume ratio, enhanced cellular uptake, and controlled drug release [3]. Among them, magnesium oxide nanoparticles (MgO NPs) have attracted attention for their bioactivity, biocompatibility, and antioxidant potential. Magnesium plays a vital role in insulin action, glucose metabolism, and enzymatic reactions related to energy production [4]. Notably, magnesium deficiency is commonly observed in individuals with type 2 diabetes and is linked to increased insulin resistance and poor glycemic control. Conventional chemical synthesis of nanoparticles, however, often involves toxic reagents and harsh conditions that pose environmental and biological risks. To address these challenges, green synthesis methods utilizing plant extracts have emerged as eco-friendly and sustainable alternatives.

* Corresponding author: N. John Sushma.

Plant-based synthesis offers several advantages, including mild reaction conditions, low cost, and the incorporation of phytochemicals that can enhance the biological functionality of nanoparticles. *Solanum lycopersicum* (tomato) is rich in bioactive compounds such as lycopene, flavonoids, and phenolic acids, which possess well-documented antioxidant, anti-inflammatory, and antidiabetic properties [5]. These phytochemicals can act as natural reducing and stabilizing agents in the green synthesis of nanoparticles while also contributing to their therapeutic activity. The present study focuses on the green synthesis and characterization of magnesium oxide nanoparticles using *Solanum lycopersicum* extract and evaluates their potential antidiabetic effect in streptozotocin-induced diabetic rats. This investigation aims to explore a novel, plant-based nanotherapeutic approach for the management of diabetes mellitus.

2. Materials and Methods

2.1. Plant and Chemical Materials

The *Solanum lycopersicum* plant was collected from the botanical garden. Chemicals were purchased from Sigma Aldrich.

2.2. Preparation of the Extract

Solanum lycopersicum fruits were collected, rinsed with distilled water, peeled, and ground into a fine paste which was filtered through a sterile funnel containing Whatman filter paper No. 1. This extract was stored at 4°C.

2.3. Spectrophotometric Analysis of Synthesized MgO NPs

MgO Nanoparticles were synthesized by adding 5 ml of plant extract to 100 ml of MgCl2, following a standardized protocol. Then, 50 ml of NaOH was slowly added, and the mixture was centrifuged at 10,000 rpm. The precipitate was calcined at 100-200 °C, and its absorbance was recorded at a wavelength range of 200 nm – 800 nm using a UV spectrophotometer [4]

2.4. Phase Contrast Microscopy

The synthesized nanoparticles were dispersed in water and shaken. A drop of this dispersion was observed with phase contrast microscope.

2.5. Analysis of Functional Groups of Nanoparticles by FTIR

99 mg of dry KBr was homogeneously mixed with 1 mg of MgO nanoparticles to make pellets of 7 mm diameter and 0.5 mm thickness. An FTIR spectrum was obtained on Alpha Bruker FT-IR spectrometer.

2.6. Particle Size and Zeta Potential Analysis

The zeta potential and size distribution of MgO nanoparticles were measured with Horiba Nano ZS. 1 mg of nanoparticles was dispersed in 1 ml of ultrapure water. This suspension was ultrasonically agitated for 60 seconds.

2.7. DPPH Assay

Samples of different concentrations (5 µg/ml, 10 µg/ml, 15 µg/ml, 20 µg/ml, 25 µg/ml) and ascorbic acid (standard) were prepared. The solution was made up to 3 ml with 0.004% DPPH (in methanol). Absorbance was measured at 517 nm [6].

2.8. Animal Selection and Grouping

Male albino rats, with an average age of 6 months and weight of 120 ± 20 g. They were divided into 3 groups:

- Group 1 (control): No treatment given.
- Group 2 (induced): Single dose of 40 mg/kg streptozotocin (intraperitoneal) to induce diabetes.
- Group 3 (induced + treated): Streptozotocin and MgO NPs (4 mg/kg, intraperitoneal).

2.9. Sampling Protocol

In all experimental rats, blood samples were collected from the tail vein. Serum samples (~150 µL) were obtained by centrifugation to analyze blood glucose, insulin, and HbA1c levels.

2.10. In vivo Biochemical Determination of Antidiabetic Activity of MgO Nanoparticles

Blood glucose was analyzed with a glucometer using blood from the rat's tail. Sampling was timed to maintain consistency, and readings were recorded. HbA1C levels were analyzed using standard ion-exchange HPLC protocol. Insulin levels were analyzed using standard immunoassay.

2.11. Histopathology

Cerebrum, cerebellum, medulla oblongata, and hippocampus tissues were harvested and preserved in 10% buffered formalin. They were sectioned (4 µm) after embedding in paraffin wax. Histopathological evaluation was performed using Hematoxylin and Eosin stains and observed under phase contrast microscope.

2.12. Behavioral Tests

- Heat hyperalgesic test: Paw withdrawal latency (PWL) of the right hind paw of rats in response to heat was measured using an infrared radiant heat apparatus. Animals were allowed to acclimatize for 5 minutes in the chamber. The plantar surface of the hind paw was exposed to the heat source, and the time taken for paw withdrawal was recorded. Baseline latency was set at 6 s, and a cut-off latency at 20 s [7]
- Tail immersion test: Hot allodynia or hyperalgesia was assessed using the tail immersion test at 42-48 °C. 5 cm distal part of the rat's tail was immersed in a water-filled container maintained at the required temperature. The duration of tail immersion was recorded, with a cut-off time of 20 seconds [8].
- Spontaneous locomotor activity test: Spontaneous motor activity was assessed using a photoactometer test. Rats were placed in an enclosed chamber (30 × 30 × 30 cm) containing 6 photocells. Interruptions of the photocell beams by the rats' movement were recorded digitally [9].
- Formalin test: The formalin test was used to assess the antinociceptive activity of the drugs. Rats were intraperitoneally administered with NPs. The dorsal surface of the right hind paw was injected with 20 µl of 5% formalin. The total time spent licking or biting the injured paw in the early phase (first 5 min) and the late phase (15 min to 40 min) was recorded using a stopwatch [10]

3. Results

3.1. Spectrophotometric Analysis

UV-Vi's spectrophotometry revealed the synthesis of magnesium oxide nanoparticles. The absorption spectrum displayed a peak range of 223-360 nm, with a maximum peak observed at 314 nm (Fig. 1), confirming the formation of MgO NPs. The calculated band gap energy was 3.94 eV, which is lower than the 7.8 eV band gap energy of bulk MgO.

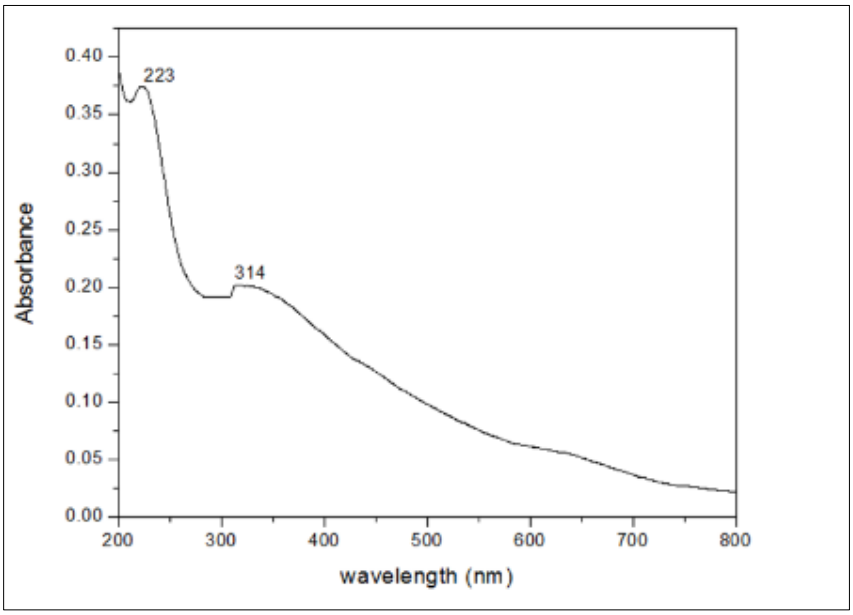

Figure 1 Absorption spectrum of green synthesized MgO NPs recorded in UV-vis spectrophotometer showing broad peak at 314 nm with low band gap energy

3.2. Phase Contrast Microscopy

Phase contrast microscopy was used for preliminary characterization. Observation at 40X magnification showed the presence of distinct particles, indicating the successful formation of nanoparticles (Fig. 2)

Figure 2 Green synthesized MgO nanoparticles observed at 40X through Phase Contrast Microscope

3.3. FTIR Analysis

FTIR spectroscopy identified the functional groups present in the synthesized nanoparticles. The spectrum showed peaks at 447.22 cm-1, 1495.90 cm-1, and 3405.61 cm-1 (Fig. 3).

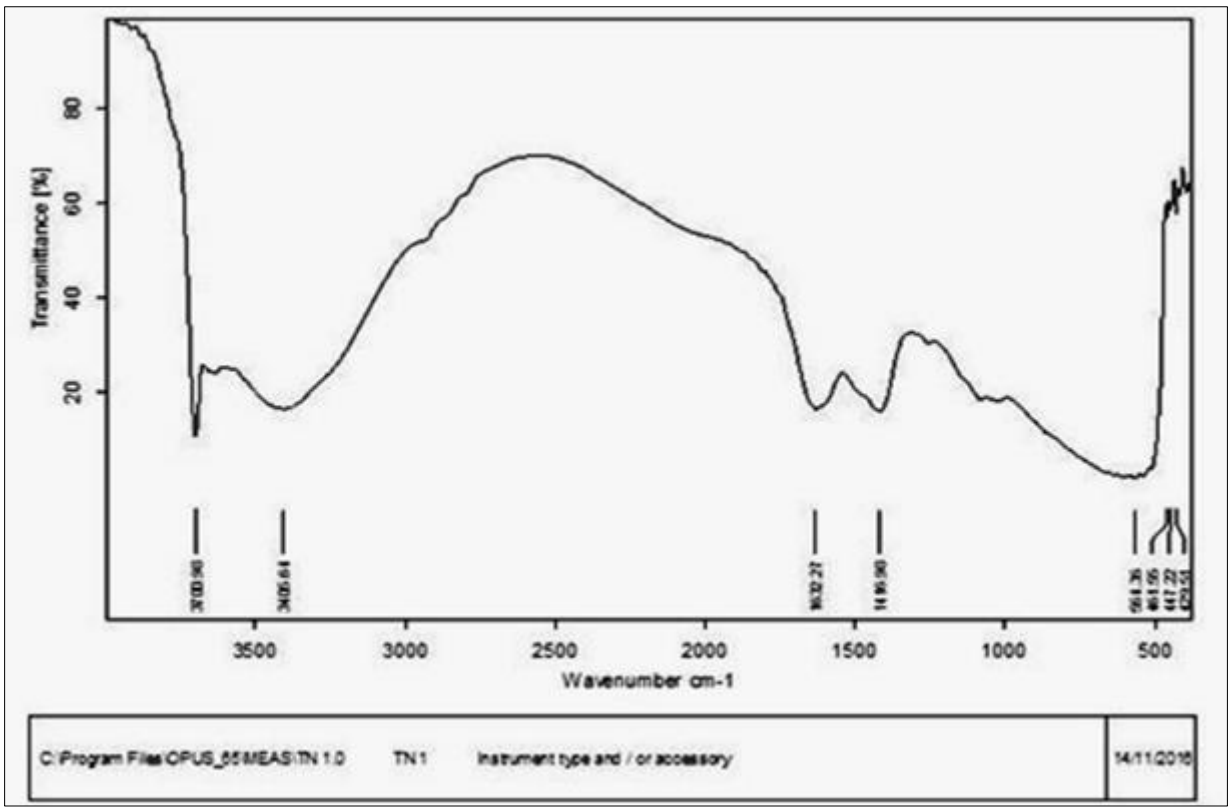

Figure 3 FTIR spectra of green synthesized MgO NPs showing peak at 447.22 cm^{-1} indicating Mg-O vibration

The peak at 447.22 cm-1 is characteristic of Mg-O stretching vibrations, confirming the formation of MgO. The peaks at 1495.90 cm-1 indicate asymmetrical and symmetrical stretching vibrations of carbonate, and the peak at 3405.61 cm-1 suggests the presence of -OH stretching.

3.4. SEM-EDS Analysis

SEM-EDS analysis provided information on the elemental composition of the synthesized nanoparticles. The analysis revealed the presence of 36.21% Mg (wt %), along with 54.47% O, 6.83% Na and 2.49% S (Fig. 4).

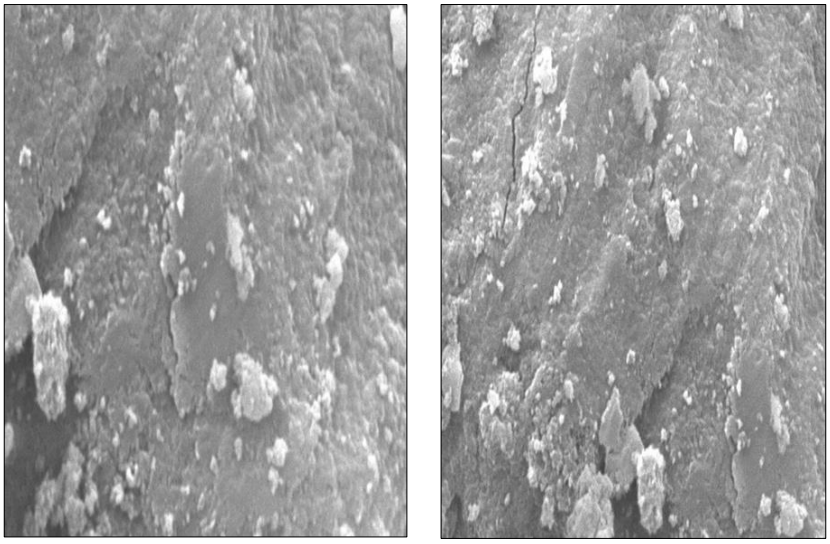

Figure 4 Visualization of green synthesized MgO NPs by SEM- EDS with 36.21% Mg (wt%)

3.5. Particle Size and Zeta Potential Analysis

Particle size analysis determined the mean particle size to be 144.1 nm, confirming the synthesis of nanoparticles (Fig. 5).

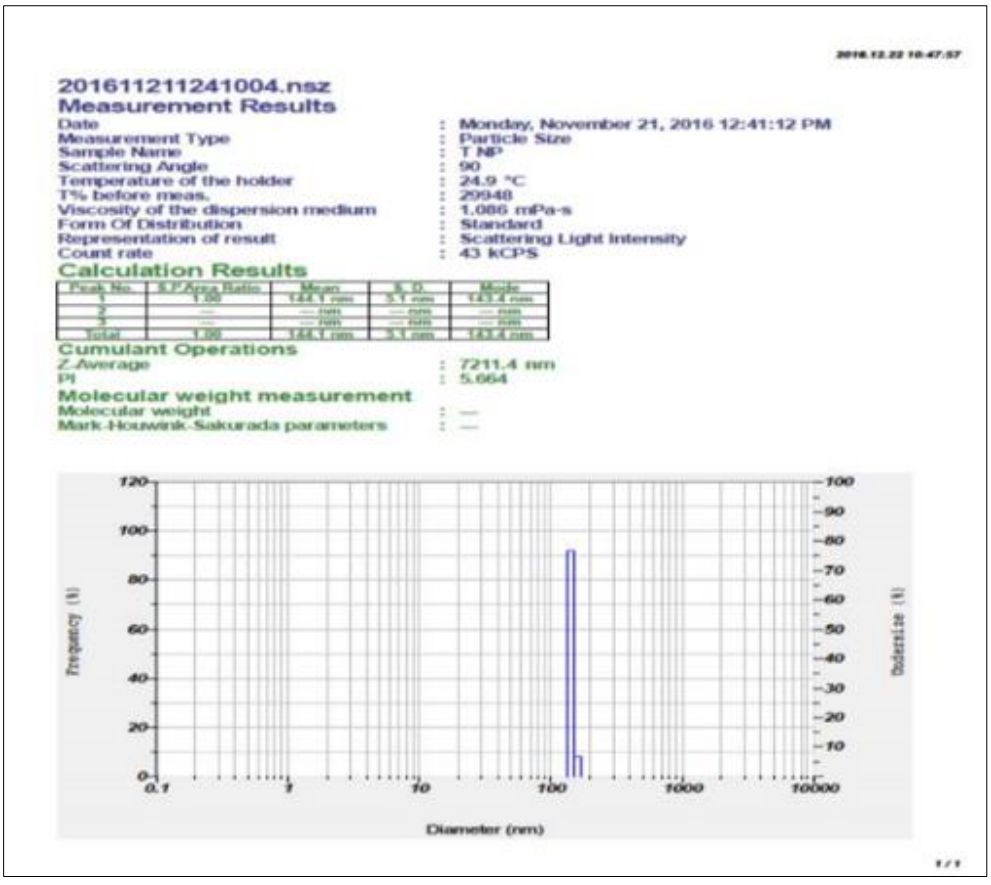

Figure 5 Graphical representation of the mean particle size of green synthesized MgO NPs at 144.1nm

Zeta potential measurement indicated a value of -19.1 mV (Fig. 6), suggesting the formation of stable particles with minimal agglomeration.

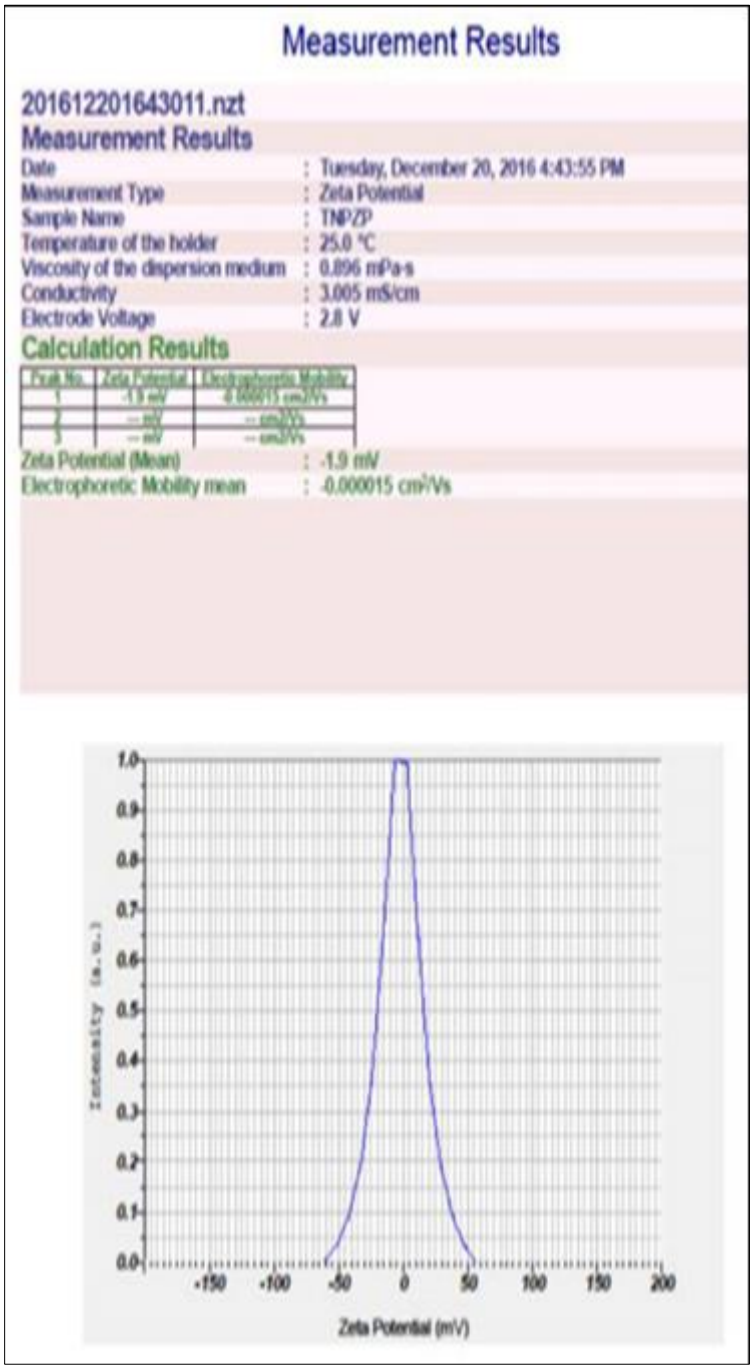

Figure 6 Graphical representation of the zeta potential of green synthesized MgO NPs at -1.9 mv

3.6. TEM Analysis

TEM analysis was used to visualize the size and shape of the nanoparticles at higher magnification. The SAED pattern revealed the polycrystalline nature of the synthesized particles, showing elongated spike-shaped structures with aggregation at the 50 nm scale (Fig. 7).

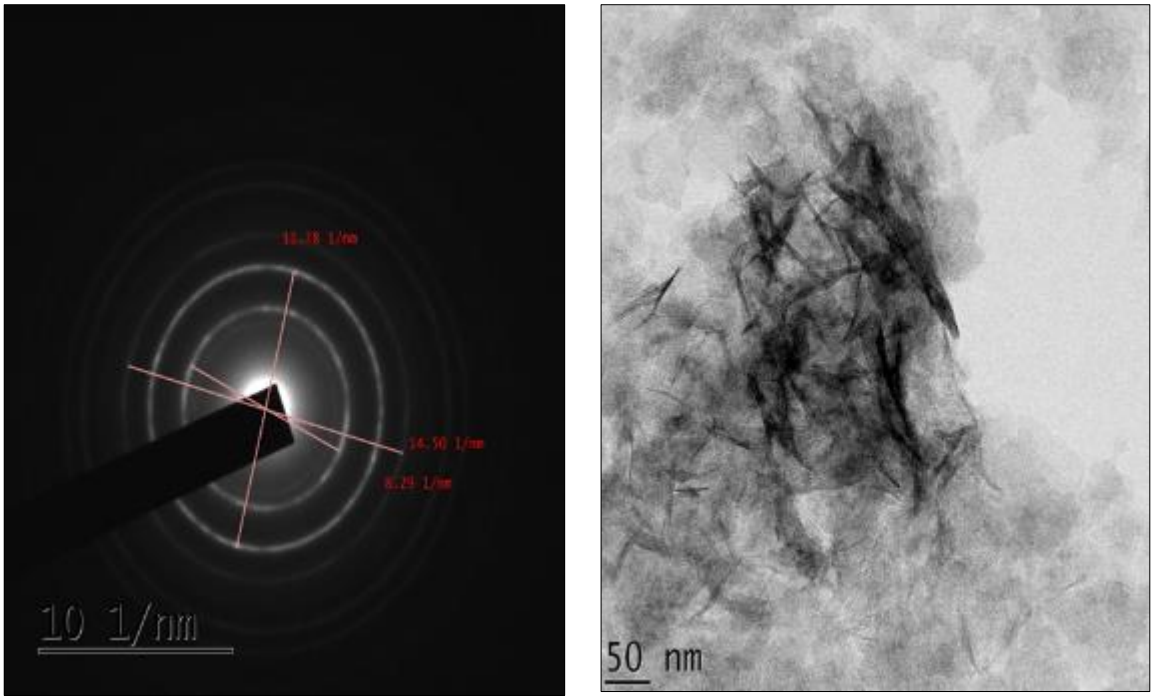

Figure 7 Visualization of green synthesized MgO NPs by TEM SAED

3.7. DPPH Assay

The antioxidant activity of the synthesized nanoparticles was evaluated using the DPPH assay. The nanoparticles exhibited 20.19% inhibition at 100 µg/ml when compared with the standard ascorbic acid (Fig. 8).

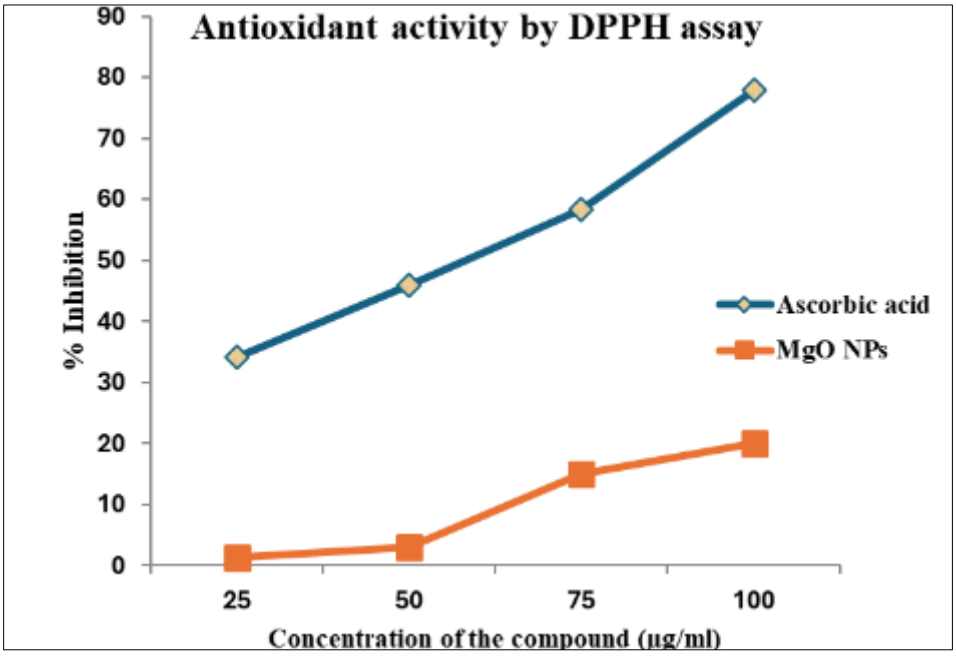

Figure 8 In vitro antioxidant activity of the green synthesized MgO nanoparticles by DPPH assay

3.8. Biochemical Analysis of Antidiabetic Activity

In vivo assessment of antidiabetic activity in rats showed significant changes in glucose, HbA1C, and insulin levels. Glucose levels in diabetic neuropathy-induced rats increased to 228.571%, HbA1C levels increased to 239.757%, and insulin levels increased to 1559.34%. Following treatment with MgO nanoparticles, glucose levels decreased to 161.905%, HbA1C levels decreased to 116.146%, and insulin levels decreased to 158.842% (Fig. 9, Table 1).

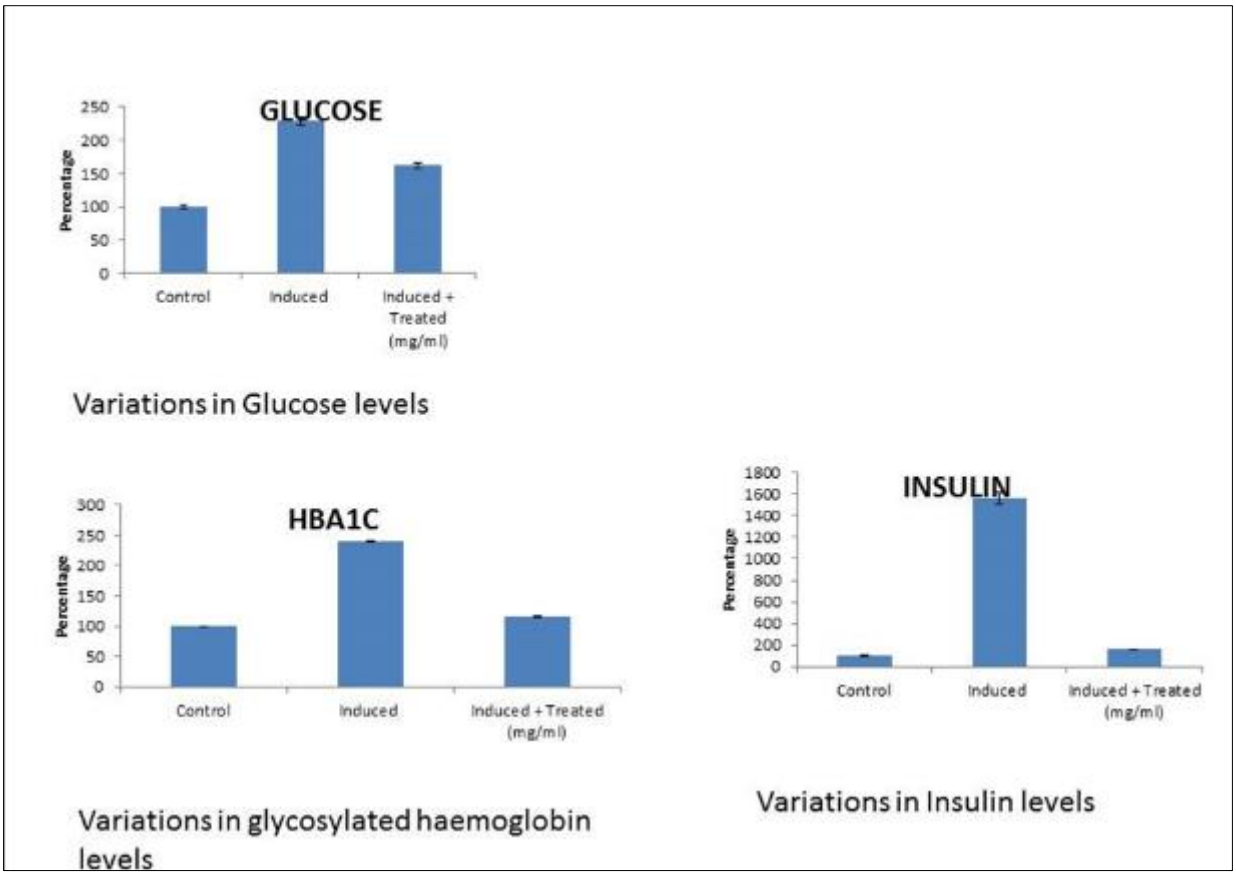

Figure 9 Biochemical analysis of antidiabetic activity of green synthesized MgO NPs

Table 1 The comparative analysis of **HbA1c levels, glucose levels, and insulin levels** across three experimental groups

Levels of HbA1c					
S.No	**Samples**	**Mean**	**%**	**SD**	**tTEST**
1	Control	5.76	100	0.02309	
2	Induced	13.81	239.757	0.28868	0.01818
3	Induced + Treated (mg/ml)	6.69	116.146	0.34641	0.21097
Levels of glucose					
S.No	**Samples**	**Mean**	**%**	**SD**	**tTEST**
1	Control	73.5	100	2.88675	
2	Induced	168	228.571	5.7735	0.05042
3	Induced + Treated (mg/ml)	119	161.905	3.4641	0.07658
Levels of insulin					
S.No	**Samples**	**Mean**	**%**	**SD**	**tTEST**
1	Control	573.8	100	5.7735	
2	Induced	8947.5	1559.34	59.4671	0.00354
3	Induced + Treated (mg/ml)	911.435	158.842	3.49297	0.01513

3.9. Histopathology

Histopathological examination of the cerebrum, cerebellum, medulla oblongata, and hippocampus of streptozotocin-induced rats revealed visible lesions. In contrast, nanoparticle-treated rats showed restoration of normal tissue structure (Figs. 10-13).

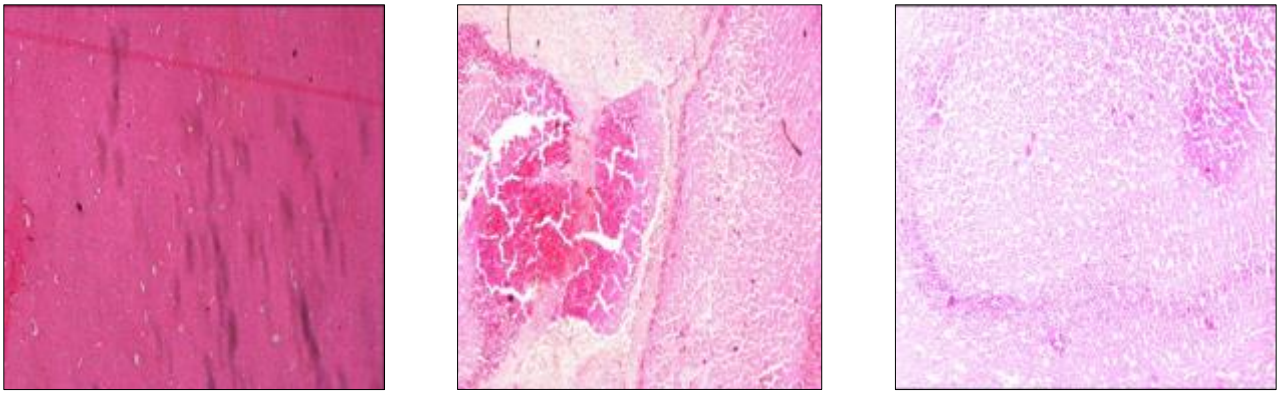

Figure 10 Photomicrograph showing – (1) Control, (2) Streptozotocin induced, (3) MgO NPs treated cerebral cortex of albino rats

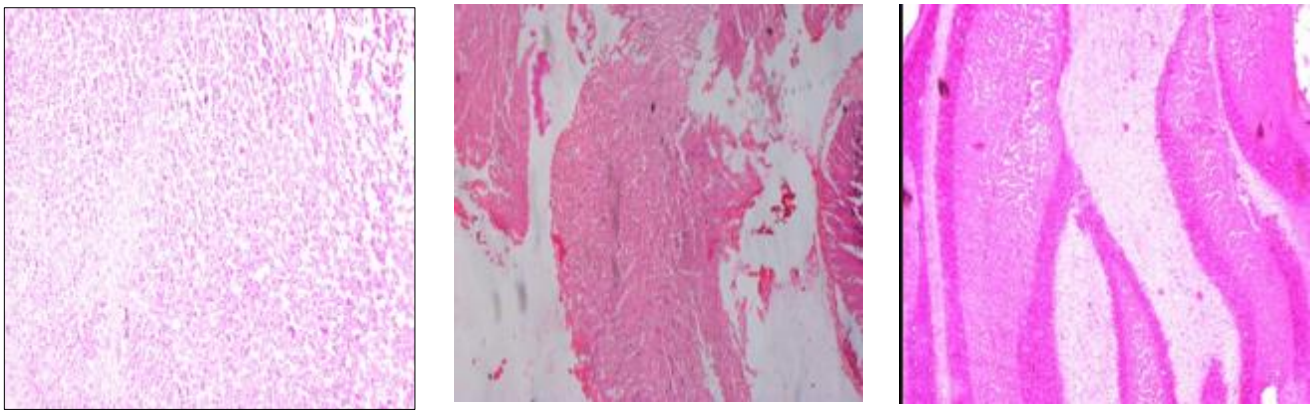

Figure 11 Photomicrograph showing – (1) Control, (2) Streptozotocin induced, (3) MgO NPs treated cerebellum of albino rats

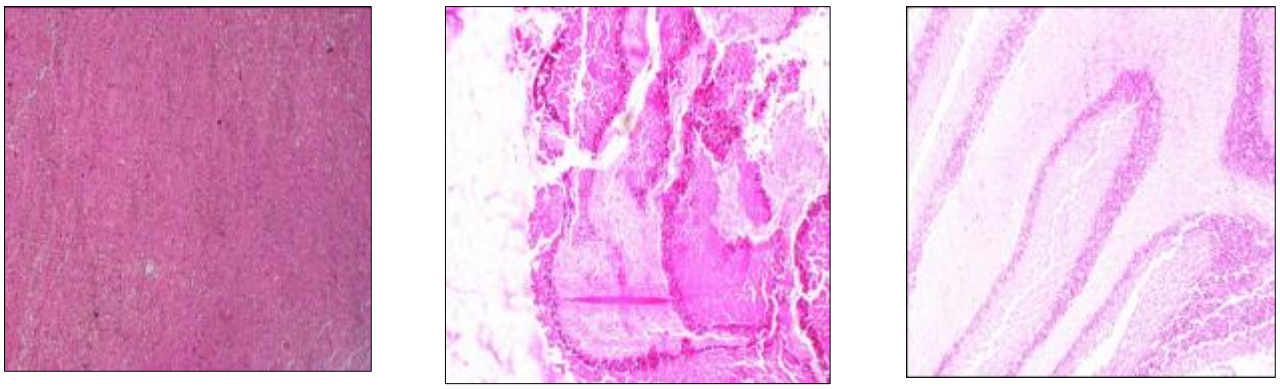

Figure 12 Photomicrograph showing – (1) Control, (2) Streptozotocin induced, (3) MgO NPs treated medulla oblongata of albino rats

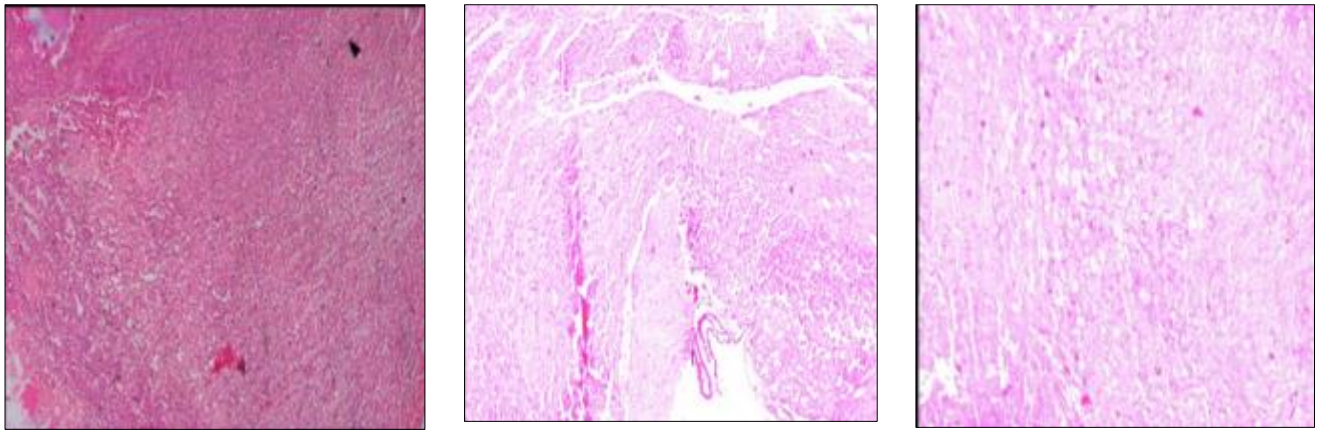

Figure 13 Photomicrograph showing – (1) Control, (2) Streptozotocin induced, (3) MgO NPs treated hippocampus of albino rats

3.10. Behavioral Tests

Behavioral tests assessed the antidiabetic neuropathic effect of the nanoparticles. In the hot plate analgesiometer test, DN-induced rats had a mean reflex time of 8 seconds, while nanoparticle-treated rats had a mean reflex time of 4.27 seconds. In the tail immersion test, DN-induced rats had a mean reflex time of 7.73 seconds, and MgO-treated rats had a mean reflex time of 3.73 seconds. The photoactometer test showed greater movement in DN-induced rats (mean of 144.27) compared to control, with nanoparticle-treated rats similar to the control group. The formalin test showed that treated rats had reduced pain behavior in both the early and late phases when compared to DN induced rats (Table 2)

Table 2 Detection of analgesia by Hot Plate Analgesiometer in Rats

S.No	Animal groups	Mean	Standard error
1	Control	5.87	0.32
2	DN induced	8	0.24
3	MgO NPs treated	4.27	0.25

Table 3 Detection of response latency by Tail Immersion Test

S.No	Animal groups	Mean	Standard error
1	Control	3.67	0.33
2	DN induced	7.73	0.45
3	MgO NPs treated	3.73	0.36

Table 4 Detection of hyperactivity by Photoactometer

S.No	Animal groups	Mean	Standard error
1	Control	133.18	5.32
2	DN induced	144.27	8.26
3	MgO NPs treated	140.93	5.64

Table 5 Detection of pain behavior by Formalin nociception test

S.No	Animal groups	Mean (phase1)	Mean (phase 2)	Standard error (phase 1)	Standard error (phase 2)
1	Control	69.27	151.15	11.55	25.42
2	DN induced	45.87	55.33	3.58	6.57
3	MgO NPs treated	74.80	148.69	9.87	18.45

4. Discussion

UV-Vis Spectrophotometry served as the preliminary method to confirm the synthesis of magnesium oxide nanoparticles (MgO NPs). As shown in Figure 1, the absorption spectrum displayed a peak range of 223–360 nm, with a prominent maximum at 314 nm, confirming the formation of MgO NPs. This observation aligns with previously reported studies [4]. The calculated band gap energy of 3.94 eV—lower than the band gap energy of bulk MgO (7.8 eV)—is consistent with earlier findings, which report a decrease in band gap energy with increasing nanoparticle size [11]. For instance, a band gap of 4.2 eV is associated with MgO NPs of approximately 28 nm size, suggesting that the particles synthesized in the current study may be larger than 28 nm, as inferred from spectrophotometric data. To visually confirm the presence of the synthesized particles, phase contrast microscopy was employed as a basic imaging tool. Figure 2 shows distinct nanoparticles observed at 40X magnification, providing preliminary evidence for their successful formation.

FTIR analysis further confirmed nanoparticle synthesis. The spectrum (Figure 3) revealed absorption peaks at 447.22 cm^{-1}, 1495.90 cm^{-1}, and 3405.61 cm^{-1}. The peak at 447.22 cm^{-1} corresponds to the characteristic Mg–O stretching vibration, indicating the presence of MgO. The peak at 1495.90 cm^{-1} was attributed to asymmetric and symmetric stretching vibrations of carbonate groups, and the broad band at 3405.61 cm^{-1} is indicative of O–H stretching vibrations. These findings are in agreement with the data reported by [12]. Additionally, a minor peak near 1400 cm^{-1}, corresponding to carboxylate vibrations, suggests the presence of trace impurities. Scanning Electron Microscopy (SEM) combined with Energy Dispersive X-ray Spectroscopy (EDS) validated the elemental composition of the sample. The analysis revealed a composition of 36.21 wt% Mg, 54.47 wt% O, along with traces of Na (6.83%), S (2.49%) confirming the predominant presence of MgO nanoparticles with high purity. Particle size analysis demonstrated an average particle size of 144.1 nm, confirming that the synthesized material falls within the nanoscale range. The zeta potential was measured at –19.1 mV, indicating good stability with minimal agglomeration due to electrostatic repulsion. Transmission Electron Microscopy (TEM) provided high-resolution imaging, showing elongated, spike-like structures with visible aggregation at the 50 nm scale. The Selected Area Electron Diffraction (SAED) pattern exhibited distinct diffraction rings, confirming the polycrystalline nature of the MgO nanoparticles [13].

The antioxidant activity of the MgO NPs was assessed using the DPPH assay, which revealed 20.19% inhibition at 100 µg/mL when compared to standard ascorbic acid, indicating decent radical-scavenging activity. For antidiabetic evaluation, streptozotocin (STZ)-induced diabetic rats were used as the in vivo model. In diabetic rats, blood glucose levels spiked to 228.57%, and HbA1c levels increased by 239.76% compared to normal control rats. Insulin levels, when measured using immunoassay, showed a significant increase of 1559.34%. Upon treatment with MgO NPs, a substantial therapeutic effect was observed. Glucose levels reduced to 161.91%, HbA1c to 116.15%, and insulin levels to 158.84%, indicating a strong restoration towards normal glycemic values.

Histopathological examination of the cerebrum, cerebellum, and medulla oblongata in STZ-induced rats revealed visible lesions, whereas the MgO NP-treated group showed restoration of normal tissue architecture, supporting the neuroprotective potential of the nanoparticles. In the hot plate test, STZ-induced rats showed a delayed response (mean latency: 8 seconds), while MgO NP-treated rats responded faster (4.27 seconds), similar to healthy controls. In the tail immersion test, the latency was 7.73 seconds in diabetic rats and 3.73 seconds in the treated group, again aligning with normal responses. The photoactometer test showed hyperactivity in STZ-induced rats (mean movements- 144.27), whereas MgO NP-treated rats exhibited movement patterns similar to controls. In the formalin-induced nociception test, diabetic rats demonstrated 69.27% pain behavior in Phase I (acute pain) and 151.15% in Phase II (chronic pain). Treated rats exhibited reduced pain responses of 58.08% in Phase I and 148.69% in Phase II, indicating an amelioration of both acute and chronic neuropathic pain symptoms. These combined results suggest that green-synthesized MgO nanoparticles possess significant antidiabetic, antioxidant, and neuroprotective effects, offering a promising approach for managing diabetes and its complications using eco-friendly nanotechnology.

5. Conclusion

We have successfully employed an eco-friendly and sustainable approach to synthesize magnesium oxide nanoparticles (MgO NPs) using *Solanum lycopersicum* extract, which acts as a natural reducing and stabilizing agent due to its rich reservoir of bioactive compounds. Spectroscopic and microscopic analyses confirmed the formation of MgO NPs with characteristic spike-like structures at the 50 nm scale and desirable physicochemical properties, including high purity and good stability. The biosynthesized MgO NPs demonstrated modest antioxidant potential and exhibited significant antidiabetic effects in streptozotocin-induced diabetic neuropathy rat models. Behavioral, biochemical, and histopathological assessments confirmed the therapeutic efficacy of the nanoparticles in restoring normal metabolic parameters and neural integrity. These findings highlight the potential of green-synthesized MgO NPs as a promising nano-therapeutic agent for managing diabetes. Further molecular investigations and long-term safety evaluations are recommended to support future clinical applications.

Compliance with ethical standards

Disclosure of conflict of interest

The authors declare that there is no conflict of interest regarding the publication of this paper.

Statement of ethical approval

All experimental procedures involving animals were conducted in accordance with the guidelines of the Committee for the Purpose of Control and Supervision of Experiments on Animals (CPCSEA). The study protocol was approved by the Institutional Animal Ethics Committee (IAEC) of Sri Padmavati Mahila Visvavidyalayam, under approval Registration No: 1677/PO/Re/S/2012/CPCSEA

References

[1] Tomic D, Harding JL, Jenkins AJ, Shaw JE, Magliano DJ. The epidemiology of type 1 diabetes mellitus in older adults. Nat Rev Endocrinol. 2025 Feb;21(2):92–104.

[2] Bhadouria N, Alam A, Kaur A. Nanotechnology-based Herbal Drug Formulation in the Treatment of Diabetes Mellitus. Current Diabetes Reviews. 2025 Jan;21(1).

[3] Ali S, Gohri S, Ali SA, Kumar M. Nanotechnology for Diabetes Management: Transforming Anti-diabetic Drug Delivery Systems. Current Pharmaceutical Research. 2025;45–59.

[4] John Sushma N, Prathyusha D, Swathi G, Madhavi T, Deva Prasad Raju B, Mallikarjuna K, et al. Facile approach to synthesize magnesium oxide nanoparticles by using Clitoria ternatea—characterization and in vitro antioxidant studies. Applied Nanoscience. 2016 Mar 1;6:437–44.

[5] Casey Nairenge MM, Ikechukwu M, Cheikhyoussef N, Hussein AA, Cheikhyoussef A. Phytochemicals from Tomato (*Solanum lycopersicum* L.) By-Products. Bioactive Phytochemicals in By-products from Bulb, Flower and Fruit Vegetables. 2025;329–46.

[6] Gulçin I, Huyut Z, Elmastaş M, Aboul-Enein HY. Radical scavenging and antioxidant activity of tannic acid. Arabian Journal of Chemistry. 2010 Jan 1;3(1):43–53.

[7] Pathak NN, Venkanna Balaganur, Madhu Cholenahalli Lingaraju, Kant V, Najeeb Latief, More AS, et al. Atorvastatin attenuates neuropathic pain in rat neuropathy model by down-regulating oxidative damage at peripheral, spinal and supraspinal levels. Neurochemistry International. 2014 Mar 1;68:1–9.

[8] Bardin L, Malfetes N, Newman-Tancredi A, Depoortère R. Chronic restraint stress induces mechanical and cold allodynia, and enhances inflammatory pain in rat: Relevance to human stress-associated painful pathologies. Behavioural Brain Research. 2009 Dec 28;205(2):360–6.

[9] Muthuraman A, Singh N. Attenuating effect of Acorus calamus extract in chronic constriction injury induced neuropathic pain in rats: an evidence of anti-oxidative, anti-inflammatory, neuroprotective and calcium inhibitory effects. BMC Complement Altern Med. 2011 Mar 22;11:24.

[10] Chang HY, Sheu MJ, Yang CH, Lu TC, Chang YS, Peng WH, et al. Analgesic Effects and the Mechanisms of Anti-Inflammation of Hispolon in Mice. Evidence-Based Complementary and Alternative Medicine. 2011;2011:1–8.

[11] Somanathan T, Krishna VM, Saravanan V, Kumar R, Kumar R. MgO Nanoparticles for Effective Uptake and Release of Doxorubicin Drug: pH Sensitive Controlled Drug Release. Journal of Nanoscience and Nanotechnology. 2016 Sep 1;16(9):9421–31.

[12] Zahir MH, Rahman MM, Irshad K, Rahman MM. Shape-Stabilized Phase Change Materials for Solar Energy Storage: MgO and Mg(OH)2 Mixed with Polyethylene Glycol. Nanomaterials. 2019 Dec;9(12):1773.

[13] Ramesh Raliya, Tarafdar JC, Choudhary K, Mal P, A. Raturi, Gautam R, et al. Synthesis of MgO Nanoparticles Using Aspergillus Tubingensis TFR-3. Journal of Bionanoscience. 2014 Feb 1;8(1):34–8.